



# Charmonium dissociation and recombination at LHC: Revisiting comovers



E.G. Ferreira

Departamento de Física de Partículas and IGFAE, Universidade de Santiago de Compostela, 15782 Santiago de Compostela, Spain

## ARTICLE INFO

### Article history:

Received 8 October 2013  
Received in revised form 31 January 2014  
Accepted 5 February 2014  
Available online 14 February 2014  
Editor: J.-P. Blaizot

## ABSTRACT

We present our results on charmonium production at the Large Hadron Collider energies within the comover interaction model. The formalism includes both comover dissociation of  $J/\psi$ 's and possible secondary  $J/\psi$  production through recombination. The estimation of this effect is made without involving free parameters. The comover interaction model also incorporates an analytic treatment of initial-state nuclear shadowing. With these tools, the model successfully describes the centrality, transverse momentum and rapidity dependence of the experimental data from PbPb collisions at the LHC energy of  $\sqrt{s} = 2.76$  TeV. We present predictions for PbPb collisions at  $\sqrt{s} = 5.5$  TeV.

© 2014 The Author. Published by Elsevier B.V. Open access under CC BY license. Funded by SCOAP<sup>3</sup>.

## 1. Introduction

Lattice QCD calculations predict that, at sufficiently large energy densities, hadronic matter undergoes a phase transition to a plasma of deconfined quarks and gluons (QGP). Substantial activity has been dedicated to the research of high-energy heavy-ion collisions in order to reveal the existence of this phase transition and to analyze the properties of strongly interacting matter in the new phase. The study of quarkonium production and suppression is among the most interesting investigations in this field since, in the presence of a QGP, the charmonium yield would be further suppressed due to color Debye screening [1]. Indeed, such an anomalous suppression was first observed in PbPb collisions at top CERN SPS energy [2]. Alternatively, the SPS experimental results could also be described in terms of final state interactions of the  $c\bar{c}$  pairs with the dense medium created in the collision, the so-called comover interaction model (CIM) [3–6]. This model does not assume thermal equilibrium and, thus, does not use thermodynamical concepts.

The theoretical extrapolations to RHIC and LHC energies were led mainly by two tendencies. On the one hand, the models that assume a deconfined phase during the collision pointed out the growing importance of secondary  $J/\psi$  production due to regeneration of  $c\bar{c}$  pairs in the plasma, the so-called *recombination*. The total amount of  $c\bar{c}$  pairs is created in hard interactions during the early stages of the collision. Then, either using kinetic theory and solving rate equations for the subsequent dissociation and recombination of charmonium [7–9], or assuming statistical coalescence at freeze-out [10–12], one obtains the final  $J/\psi$  yield. On the other hand, the CIM with only dissociation of  $J/\psi$ 's predicted [13] a stronger suppression at RHIC than at SPS due to a larger density of

produced soft particles in the collision. It also predicted a stronger suppression at mid-rapidity – where the comover density is maximal – than at forward rapidities. Nevertheless, measurements of  $J/\psi$  production in AuAu collisions at  $\sqrt{s} = 200$  GeV displayed surprising results: the suppression at mid-rapidity was on the same level as at SPS [14,15]. Furthermore, the suppression at forward rapidity in AuAu collisions was stronger than at mid-rapidity for the same collision energy.

These facts demonstrated that in the CIM, which is based on the well-known gain and loss differential equations in transport theory, the introduction of a recombination term is actually required for a comprehensive adjustment [16]. In the present work we use the updated version of the CIM [16], that allows recombination of  $c\bar{c}$  pairs into secondary  $J/\psi$ 's. We will estimate this effect by using the density of charm in proton-proton collisions at the same energy. Therefore, the model does not involve any additional parameter. We will proceed as follows. In Section 2 we remember the details of the model; the effects related to the initial-state shadowing and nuclear absorption, together with comover dissociation and regeneration are described. In Section 3 we present our results for PbPb collisions at the LHC energy of  $\sqrt{s} = 2.76$  TeV and predictions at  $\sqrt{s} = 5.5$  TeV. Note that, at these energies, the CIM should not be considered to describe a final-state interaction at the hadronic level. Indeed, at small values of the proper time these comovers should be considered as a dense partonic medium. Conclusions and final remarks are given in Section 4.

## 2. Description of the model

Let us briefly recall the main ingredients of the CIM. The present version of the model contains an analytic treatment of

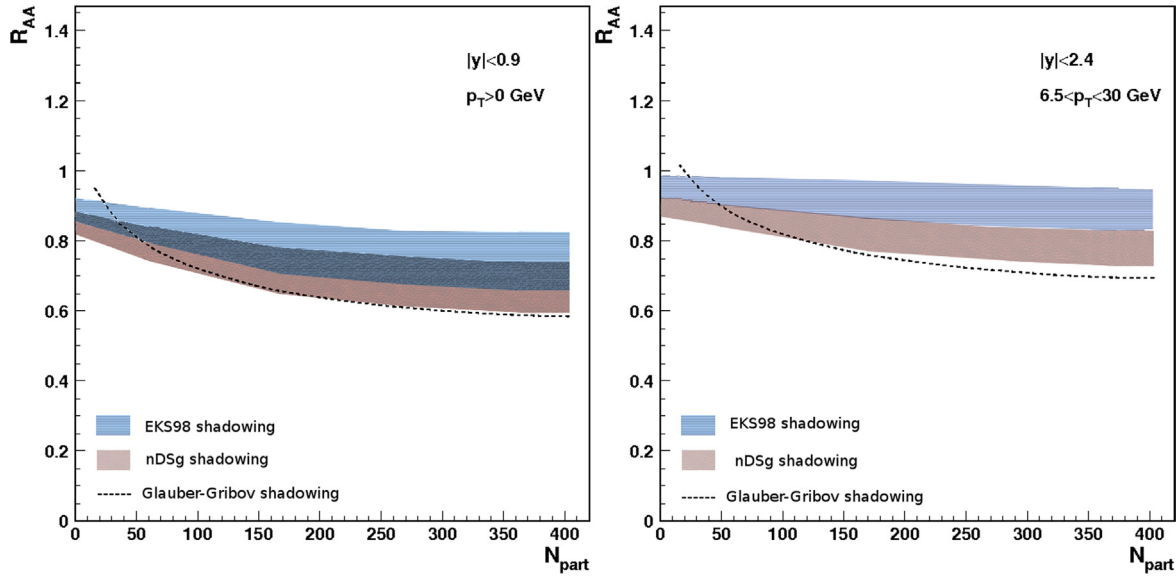


**Fig. 1.** (Color online.) Centrality dependence of the Glauber–Gribov shadowing corrections for the  $J/\psi$  compared to EKS98/nDSg calculations performed according to [27,28] in PbPb collisions at  $\sqrt{s} = 2.76$  TeV. The bands for the EKS98/nDSg models shown in the figure correspond to the uncertainty in the factorization scale. This uncertainty has not been included in the Glauber–Gribov model, where the scale corresponds to the transverse mass.

initial-state nuclear effects – the so-called *nuclear shadowing*, together with the multiple scattering of the pre-resonant  $c\bar{c}$  pair escaping the nuclear environment – the *nuclear absorption*. The specific characteristics of the model are the *interaction with the co-moving matter* and the *recombination of  $c\bar{c}$  into secondary  $J/\psi$ 's*.

The suppression of the  $J/\psi$  is usually expressed through the *nuclear modification factor*,  $R_{AB}^{J/\psi}(b)$ , defined as the ratio of the  $J/\psi$  yield in AB and  $pp$  scaled by the number of binary nucleon–nucleon collisions,  $n(b)$ . We have then

$$R_{AB}^{J/\psi}(b) = \frac{dN_{AB}^{J/\psi}/dy}{n(b) dN_{pp}^{J/\psi}/dy} = \frac{\int d^2s \sigma_{AB}(b) n(b, s) S^{abs}(b, s) S^{sh}_{J/\psi}(b, s) S^{co}(b, s)}{\int d^2s \sigma_{AB}(b) n(b, s)}, \quad (1)$$

where  $\sigma_{AB}(b) = 1 - \exp[-\sigma_{pp} AB T_{AB}(b)]$ ,  $T_{AB}(b) = \int d^2s T_A(s) \times T_B(b-s)$  is the nuclear overlap function and  $T_A(b)$  is the nuclear profile function, obtained from Woods–Saxon nuclear densities [17].

The number of binary nucleon–nucleon collisions at impact parameter  $b$ ,  $n(b)$ , is obtained upon integration over  $d^2s$  of  $n(b, s)$ :

$$n(b, s) = \sigma_{pp} AB T_A(s) T_B(b-s) / \sigma_{AB}(b). \quad (2)$$

The three additional factors in the numerator of Eq. (1),  $S^{abs}$ ,  $S^{sh}$  and  $S^{co}$ , denote the effects of nuclear absorption, shadowing and interaction with the co-moving matter – both dissociation and recombination – respectively. Any of these effects on  $J/\psi$  production will lead to a deviation of  $R_{AB}^{J/\psi}$  from unity.

It is commonly assumed that the nuclear absorption can be safely considered as negligible at the LHC [18–20] and thus we will take  $S^{abs} = 1$  for the remainder of the discussion.

## 2.1. Shadowing

Coherence effects will lead to nuclear shadowing for both soft and hard processes at high energy, and therefore also for the production of heavy flavor. Shadowing can be calculated within the Glauber–Gribov theory [21] making use of the generalized

Schwimmer model of multiple scattering [22]. The second suppression factor in Eq. (1) is then given by

$$S^{sh}(b, s, y) = \frac{1}{1 + AF(y_A)T_A(s)} \frac{1}{1 + BF(y_B)T_B(b-s)}, \quad (3)$$

where the function  $F(y)$  encodes the dynamics of shadowing. Following the spirit of the model presented in [23,24], where shadowing corrections are given without free parameters in terms of the triple-Pomeron coupling determined from diffractive data, one can write:

$$F(y) = 4\pi \int_{y_{min}}^{y_{max}} dy \frac{1}{\sigma_P(y)} \frac{d\sigma^{PPP}}{dy dt} \Big|_{t=0} = G^{PPP} [\exp(\Delta \times y_{max}) - \exp(\Delta \times y_{min})] / \Delta. \quad (4)$$

It represents the coherence effects due to the shadowing corrections expressed as the ratio of the triple-Pomeron cross section over the single-Pomeron exchange. We take  $y_{min} = \ln(R_A m_N / \sqrt{3})$  where  $m_N$  is the nucleon mass and  $R_A = (0.82 A^{1/3} + 0.58)$  fm – the Gaussian nuclear radius. The value of  $y_{max}$  depends on the rapidity  $y$  of the considered particle – the  $J/\psi$  according to Eq. (1), the energy through  $s_{NN}$  and the mass and the transverse momentum of the produced particle through the transverse mass  $m_T$ ,  $y_{max} = \ln(s_{NN}/m_T^2)/2 \pm y$  with the + (–) sign if the particle is produced in the hemisphere of nucleus B (A). We have used  $\Delta = 0.13$  and  $G^{PPP} = 0.04$  fm<sup>2</sup> ( $G^{PPP}/\Delta = 0.31$  fm<sup>2</sup>) corresponding to the Pomeron intercept  $\alpha_P(0) = 1.13$ . The scale dependence of the shadowing appears in the expression of  $y_{max}$ , through the transverse mass  $m_T$ . As a consequence, the shadowing corrections depend on the nature of the studied particle through its mass, and on its transverse momentum  $p_T$ .

Note that the above expression for the shadowing, Eq. (3), can be applied to light and heavy particles, the difference between them coming from  $y_{max}$  through the transverse mass  $m_T$ .

With the shadowing resulting from the above equations a good description of the centrality dependence of charged multiplicities is obtained both at RHIC [25] and LHC [26] energies. Concerning heavy quarks, this shadowing roughly agrees with EKS98/nDSg predictions [27–31]. In Fig. 1 we show the comparison of the

shadowing model applied here with some recent calculations developed within the framework of Refs. [27,28]. One can see that the Glauber–Gribov inspired model agrees with the lowest band of nDSg according to [27,28]. In fact, our minimum bias shadowing is of the order of 0.66, to be compared to a minimal and maximal values of 0.65–0.77 for nDSg shadowing and 0.70–0.84 for EKS98. Moreover, calculations of the shadowing developed at leading order within the framework of the Color Evaporation model [31] lead in general to a slightly higher suppression than [27]. Because of this, one can consider that the shadowing presented here agrees with the models mentioned above within uncertainties.

Note that while the particle production at SPS is dominated by low-energy effects, i.e. nuclear absorption, the RHIC domain already belongs to the high-energy regime, where nuclear shadowing becomes relevant, and the combined effect of shadowing and energy-momentum conservation should be accounted for at forward rapidities. At LHC, shadowing is expected to be strong while nuclear absorption is a small effect that can be neglected. We will now proceed with the discussion of the specific comover-interaction effects.

## 2.2. Dissociation by comover interaction and recombination

The CIM was originally developed in the nineties in order to explain both the suppression of charmonium yields [3–6,13,32,33] and the strangeness enhancement [34,35] in nucleus–nucleus collisions at the SPS. At those energies, where the recombination effects are negligible, the rate equation governing the density of charmonium in the final state,  $N_{J/\psi}$ , can be written in a simple form assuming a pure longitudinal expansion of the system and boost invariance. The density of  $J/\psi$  at a given transverse coordinate  $s$ , impact parameter  $b$  and rapidity  $y$  is then given by

$$\tau \frac{dN_{J/\psi}}{d\tau}(b, s, y) = -\sigma_{co} N^{co}(b, s, y) N_{J/\psi}(b, s, y), \quad (5)$$

where  $\sigma_{co}$  is the cross section of charmonium dissociation due to interactions with the co-moving medium, with density  $N^{co}$ . It was fixed from fits to low-energy experimental data to be  $\sigma_{co} = 0.65$  mb [5].

In order to incorporate the effects of recombination, one has to include an additional gain term proportional to the squared density of open charm produced in the collision. Eq. (5) is then generalized to

$$\tau \frac{dN_{J/\psi}}{d\tau}(b, s, y) = -\sigma_{co} [N^{co}(b, s, y) N_{J/\psi}(b, s, y) - N_c(b, s, y) N_{\bar{c}}(b, s, y)], \quad (6)$$

where we have assumed that the effective recombination cross section is equal to the dissociation cross section. Note that these two cross sections have to be similar but not necessarily equal. We have taken the simplest possibility. Therefore, the extension of the model conducing to include recombination does not involve additional parameters.<sup>1</sup> All the densities involved in Eq. (6) are assumed to decrease as  $1/\tau$ . The approximate solution of Eq. (6) is given by

$$S^{co}(b, s, y) = \exp \left\{ -\sigma_{co} \left[ N^{co}(b, s, y) - \frac{N_c(b, s, y) N_{\bar{c}}(b, s, y)}{N_{J/\psi}(b, s, y)} \right] \times \ln \left[ \frac{N^{co}(b, s, y)}{N_{pp}(0)} \right] \right\}, \quad (7)$$

<sup>1</sup> Strictly speaking, the equivalence between breakup and recombination cross sections only holds if one consider the direct  $J/\psi$  production. Considering the feed down in a detailed way can induce differences between both interaction cross sections.

where the first term in the exponent corresponds to the exact solution of Eq. (5), i.e. the survival probability of a  $J/\psi$  interacting with comovers [13]. The breakup and recombination in the above equation do not need to occur on the same time. The density of comovers is calculated following the same lines as in [26] together with the shadowing correction:

$$N^{co}(b, s, y) = N_{NS}^{co}(b, s, y) S_{ch}^{sh}(b, s, y), \quad (8)$$

where  $S_{ch}^{sh}$  denotes the shadowing for light particles, calculated according to Eq. (3). The non-shadowed (NS) multiplicity of comovers is taken as proportional to the number of nucleon–nucleon collision according to Eq. (2)

$$N_{NS}^{co}(b, s, y) = N^{pp}(b, s, y) n(b, s), \quad (9)$$

where  $N^{pp}$  represents the comover density in  $pp$  collisions, essentially  $N^{pp}(y) = \frac{3}{2} (dN^{ch}/dy)^{pp}$ . In fact, when using at mid-rapidity the value  $(dN^{ch}/d\eta)_{y=0}^{pp} = 3.8$ , i.e. the inelastic value of  $dN^{pp}/d\eta$  at  $\sqrt{s} = 2.76$  TeV, a good agreement with experimental data on charged particle multiplicities is obtained [26].

The density of open and hidden charm in AA collisions,  $N_c$ ,  $N_{\bar{c}}$  and  $N_{J/\psi}$ , respectively, can be computed from their densities in  $pp$  collisions as  $N_c^{AA}(b, s) = n(b, s) S_{HQ}^{sh}(b, s) N_c^{pp}$ , with similar expression for  $N_{\bar{c}}^{AA}$  and  $N_{J/\psi}^{AA}$ . Here  $n(b, s)$  is given by Eq. (2) and  $S_{HQ}^{sh}$  is the shadowing factor for heavy quark production, given by Eq. (3). Eq. (7) becomes

$$S^{co}(b, s, y) = \exp \left\{ -\sigma_{co} [N^{co}(b, s, y) - C(y) n(b, s) S_{HQ}^{sh}(b, s)] \times \ln \left[ \frac{N^{co}(b, s, y)}{N_{pp}(0)} \right] \right\} \quad (10)$$

where

$$C(y) = \frac{(dN_c^{pp}/dy)(dN_{\bar{c}}^{pp}/dy)}{dN_{J/\psi}^{pp}/dy} = \frac{(dN_{c\bar{c}}^{pp}/dy)^2}{dN_{J/\psi}^{pp}/dy} = \frac{(\sigma_{pp}^{c\bar{c}}/dy)^2}{\sigma_{pp}^{J/\psi}/dy}. \quad (11)$$

The quantities in the rightmost term in Eq. (11) are all related to  $pp$  collisions at the corresponding energy. The value for  $d\sigma_{pp}^{J/\psi}/dy$  can be taken from experimental data [36] or from a model for extrapolation of the experimental results [37]. The  $c\bar{c}$  pairs are mostly in charmed mesons, such as  $D$  and  $D^*$  and the corresponding values could be extracted from the experiment [38], leading to an estimation of  $d\sigma_{pp}^{c\bar{c}}/dy$ , as we will discuss below. For  $\sigma_{pp}$  we use the non-diffractive value  $\sigma_{pp} = 54$  mb [26] at  $\sqrt{s_{NN}} = 2.76$  TeV.

With  $\sigma_{co}$  fixed from experiments at low energy, where recombination effects are negligible, the model, formulated above, should be self-consistent at high energies. Note, however, that  $\sigma_{co}$  could change when the energy increases. We do not expect this effect to be important and, since we are unable to evaluate the magnitude of this eventual change, we have used the same value  $\sigma_{co} = 0.65$  mb at all energies.

## 3. Results

Our results for the centrality dependence of the  $J/\psi$  nuclear modification factor in PbPb collisions at 2.76 TeV are presented in Fig. 2 compared to ALICE experimental data [39–42] at mid and forward rapidities. The different contributions to  $J/\psi$  suppression are shown. Note that the initial-state effect is just the shadowing, which can induce a suppression of  $R_{AA} = 0.6$  for the more central

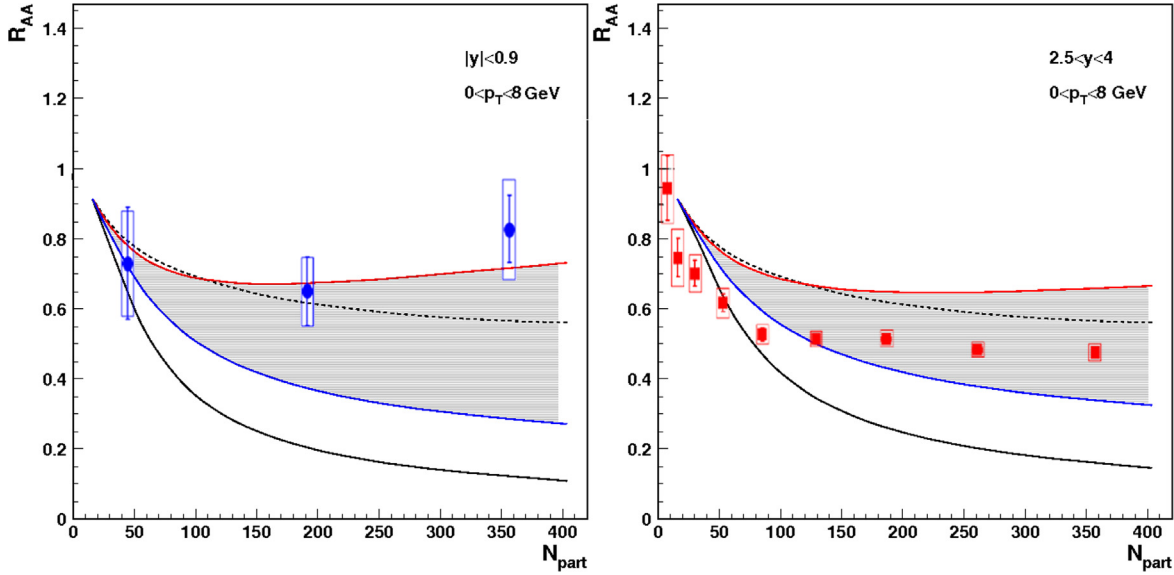


**Fig. 2.** (Color online.) Results on the centrality dependence of the  $J/\psi$  nuclear modification factor in PbPb collisions at 2.76 TeV at mid (left) and forward (right) rapidity compared to ALICE data [39–42]. The dashed line corresponds to the *shadowing* effect on the  $J/\psi$ . The lowest continuous line (black) corresponds to the combined effect of the *shadowing* and the *comover dissociation*. The shadowed area corresponds to our result when the *shadowing*, the *comover dissociation* and the *recombination* are taken into account. The uncertainty takes into account the variation between the minimum (blue line) and maximal (red line) values of  $C(y)$ .

collisions [28]. The combined effect of shadowing and comover dissociation gives a too strong suppression compared to experimental data. We therefore proceed to estimate the effect of recombination.

For the charmonium cross section  $pp$  measurements around mid-rapidity are available from ALICE [36] at 2.76 TeV which corresponds to  $\frac{d\sigma_{pp}^{J/\psi}}{dy} = 3.73 \mu\text{b}$ . We consider that realistic values of  $C(y)$  at mid-rapidity at 2.76 TeV are in the range of a minimum value of 2 up to a maximal value of 3 which corresponds to a cross section  $\frac{d\sigma_{pp}^{cc}}{dy} \approx 0.6\text{--}0.8 \text{ mb}$ . This agrees with the estimated values in [43], and corresponds to a  $\sigma_{cc}^{tot}$  around 5 mb, which agrees well with experimental data [38]. These values are higher than the ones reported in [44], where data is also reproduced. Note nevertheless that there is no contradiction, since in [44] the initial-state shadowing is not considered. This shadowing, that affects also heavy flavors, would imply an extra suppression leading naturally to the choice of higher input charm cross sections  $d\sigma_{pp}^{cc}/dy$ . In other words, one can consider that in the approach developed in [44] the choice of smaller  $\frac{d\sigma_{pp}^{cc}}{dy}$ ,  $\frac{d\sigma_{pp}^{cc}}{dy} \approx 0.3\text{--}0.4 \text{ mb}$ , takes into account an effect of shadowing that reduces the input cross section up to 1/2.

We expect the effect of recombination to be stronger at mid than at forward rapidities. At  $y \neq 0$  the recombination term is smaller since the rapidity distribution of  $D$ ,  $D^*$  is narrower than the one of comovers, which induces a decrease of the  $C(y)$ -value. This will produce a decrease of  $R_{AA}^{J/\psi}$  with increasing  $y$ . Note nevertheless that this effect may be compensated by the increase of  $R_{AA}^{J/\psi}$  due to a smaller density of comovers at  $y \neq 0$ , which induces less dissociation. We have chosen a smooth behavior of  $C(y)$  with rapidity, which in the rapidity range  $2.5 < y < 4$  corresponds to a mean reduction in the  $C(y)$ -value of the order of 20%. Taking  $\frac{d\sigma_{pp}^{J/\psi}}{dy}$  in this forward rapidity range,  $\frac{d\sigma_{pp}^{J/\psi}}{dy} = 2.23 \mu\text{b}$  [36], these  $C(y)$ -values correspond to an input charm cross section  $\frac{d\sigma_{pp}^{cc}}{dy} \approx 0.4\text{--}0.6 \text{ mb}$  in the forward rapidity region. Our procedure gives a reasonable description of data when recombination is taken into account.

Some considerations apply here.

First, the behavior of the nuclear modification factor  $R_{AA}^{J/\psi}$  for different rapidity ranges changes depending of the amount of recombination considered. If the recombination  $C(y)$ -value is considered to be small – lower limit – the total suppression will be controlled essentially by the comover dissociation, and the nuclear modification factor will follow the same behavior as the usual comover suppression, but with a higher absolute value. On the other hand, when the  $C(y)$ -value is taken as its upper limit, the recombination term controls the total suppression, inducing a decrease of the nuclear modification factor when going to forward rapidities.

Second, the shadowing corrections for heavy quarks we use here have been calculated in a very simple way, according to Eq. (3) within the Glauber–Gribov theory. The advantage is that all calculations can be easily done analytically. This shadowing roughly agrees with EKS98/nDSg predictions, as shown in Fig. 1, in particular in the mid-rapidity region. Nevertheless, the Glauber–Gribov shadowing is almost constant with rapidity. Even if the  $y$ -dependence of the different shadowing models in AA collisions and in the rapidity ranges here considered is quite flat, as it shown in [39] and Refs. [28,31] therein, we are aware that our approach can induce an small overestimation of the shadowing suppression in the forward rapidity region. In fact we contemplate the upgrading of the CIM by the introduction of EKS98/nDSg/EPS09 according to [28,27,45].

We proceed now to study the behavior of the nuclear modification factor when different transverse momentum cuts are introduced. In order to avoid an unnecessary complication of the notation, the explicit  $p_T$  dependence is not shown in our equations. The  $p_T$  comover distribution follows essentially the lines of reference [46]. Moreover, the  $p_T$  dependence also enter through the shadowing – both on the  $J/\psi$  and the comovers. The main effect would be smaller shadowing suppression for the comovers a high  $p_T$ , which leads to stronger  $J/\psi$  suppression at high  $p_T$  due to comover interaction. This effect is not compensate by the smaller shadowing corrections that affect the  $J/\psi$ , since the higher mass of the  $c\bar{c}$  pair makes the shadowing difference between the low and high  $p_T$  regions less important than for the case of the comovers. A detail work will be developed in [47].



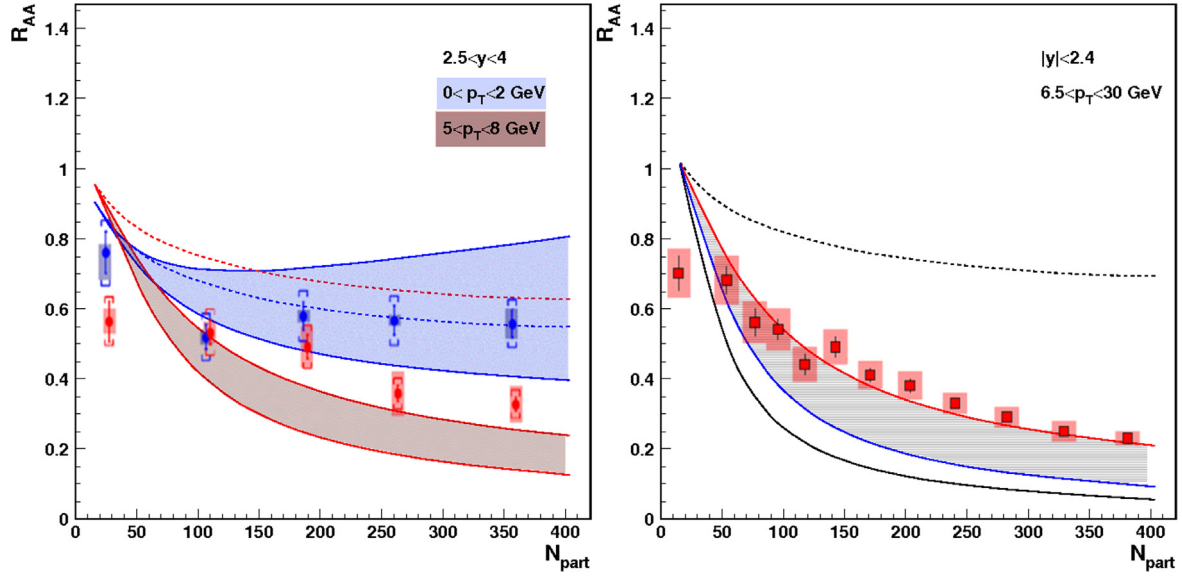


**Fig. 3.** (Color online.) Results on the centrality dependence of the  $J/\psi$  nuclear modification factor in PbPb collisions at 2.76 TeV compared to ALICE forward rapidity data [42] in the  $p_T$  ranges  $0 < p_T < 2$  GeV and  $5 < p_T < 8$  GeV (left) and compared to CMS mid-rapidity data [48–50] in the  $p_T$  range  $6.5 < p_T < 30$  GeV (right). The dashed line corresponds to the *shadowing* effect on the  $J/\psi$ . The lowest continuous line (black) in the right figure corresponds to the combined effect of the *shadowing* and the *comover dissociation*. The shadowed areas correspond to our result when the *shadowing*, the *comover dissociation* and the *recombination* are taken into account. The uncertainty takes into account the variation between the minimum and maximal values of  $C(y)$ .

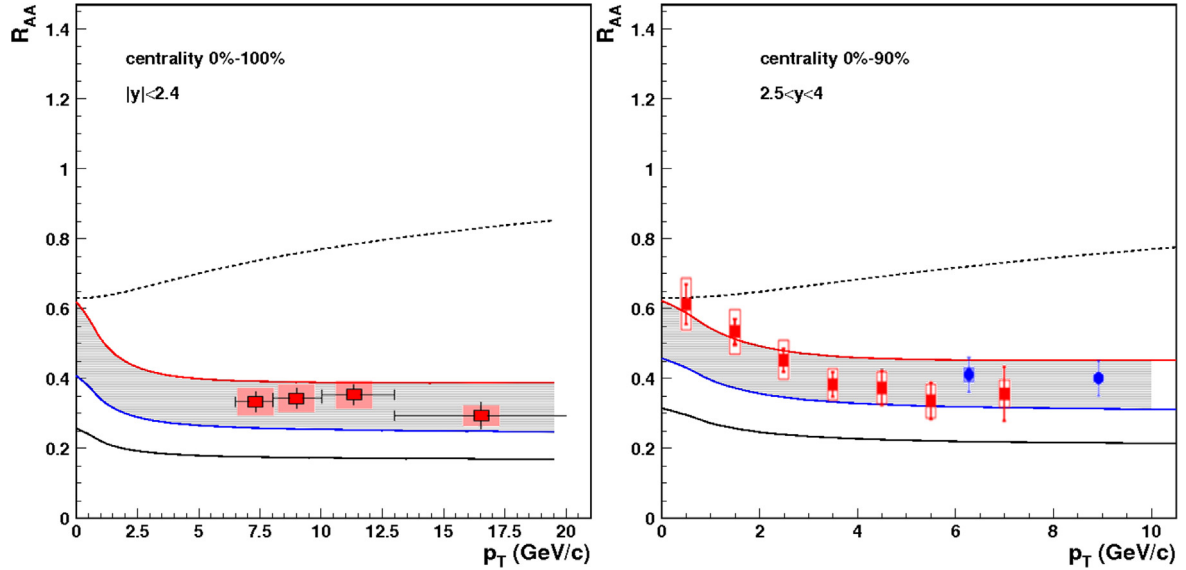


**Fig. 4.** (Color online.) Results on the transverse dependence of the  $J/\psi$  nuclear modification factor in PbPb collisions at 2.76 TeV compared to CMS data [48,49] at mid-rapidity (left) and to ALICE [42] and CMS data [48] at forward rapidity (right). The CMS data on the left part of the figure corresponds to the rapidity range  $1.6 < |y| < 2.4$ , while the ALICE data lie in the range  $2.5 < y < 4$ . The dashed line corresponds to the *shadowing* effect on the  $J/\psi$ . The lowest continuous line (black) corresponds to the combined effect of the *shadowing* and the *comover dissociation*. The shadowed area corresponds to our result when the *shadowing*, the *comover dissociation* and the *recombination* are taken into account. The uncertainty takes into account the variation between the minimum (blue line) and maximal (red line) values of  $C(y)$ .

In Fig. 3 (left) our results for 2 different  $p_T$  ranges,  $0 < p_T < 2$  GeV and  $5 < p_T < 8$  GeV, are compared to ALICE forward rapidity data [42]. Clearly, the amount of recombination is more important in the low  $p_T$  region. The comparison to CMS data at mid-rapidity and higher  $p_T$ ,  $6.5 < p_T < 30$  GeV [48–50], in Fig. 3 (right) emphasizes this finding: the amount of recombination is much smaller than in the mid-rapidity range at low  $p_T$ , as shown in Fig. 2 (left). It is important to point out that this experimental fact – stronger suppression at higher  $p_T$  – cannot be due to initial-state shadowing effects on the  $J/\psi$ : the presence of shadowing corrections, more relevant at lower  $p_T$ , acts in the opposite direction.

Moreover, our results on the dependence of the  $J/\psi$  nuclear modification factor on the transverse momentum are shown in Fig. 4 compared to CMS [48,49] and ALICE [41] data. An overall agreement is obtained.

We continue by showing our results versus rapidity. In Fig. 5 (left) we compare our results with CMS data [48,49] in the mid-rapidity region. An overall agreement is obtained. The fact that we do not reproduce the detailed behavior of ALICE data [41], as can be seen in Fig. 5 (right), is extremely instructive. As we have mentioned above, we have chosen a very conservative behavior of  $C(y)$  with rapidity, which leads to a mean reduction in the  $C(y)$ -value of the order of 20% in the rapidity range  $2.5 < y < 4$ .

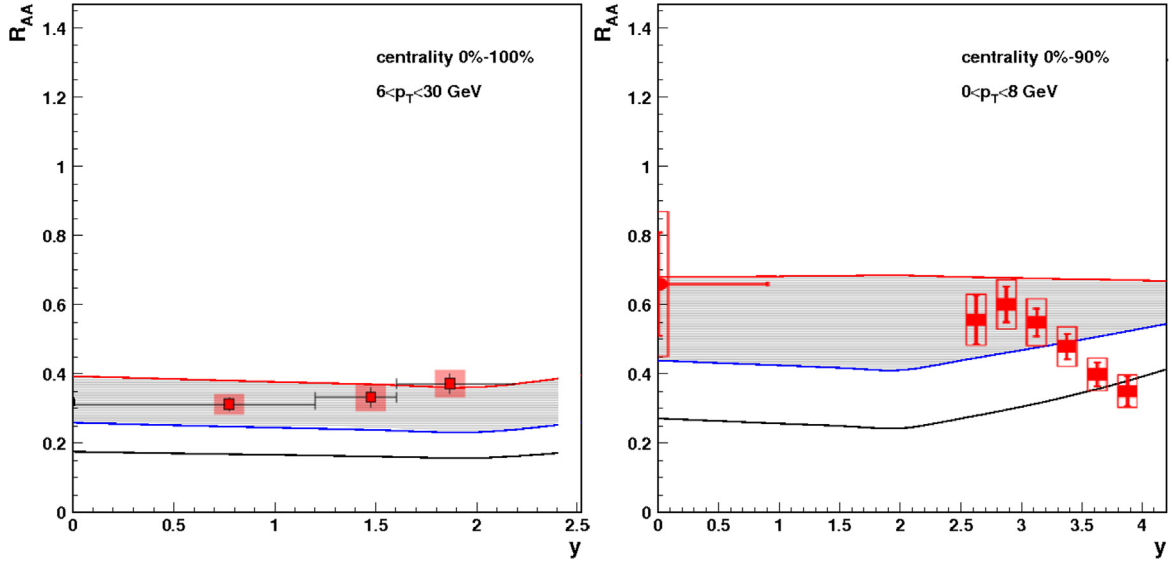


**Fig. 5.** (Color online.) Results on the rapidity dependence of the  $J/\psi$  nuclear modification factor in PbPb collisions at 2.76 TeV compared to CMS data [48,49] at mid-rapidity (left) and to ALICE [41] at mid and forward rapidity (right). The dashed line corresponds to the shadowing effect on the  $J/\psi$ . The lowest continuous line (black) corresponds to the combined effect of the shadowing and the comover dissociation. The shadowed area corresponds to our result when the shadowing, the comover dissociation and the recombination are taken into account. The uncertainty takes into account the variation between the minimum (blue line) and maximal (red line) values of  $C(y)$ .

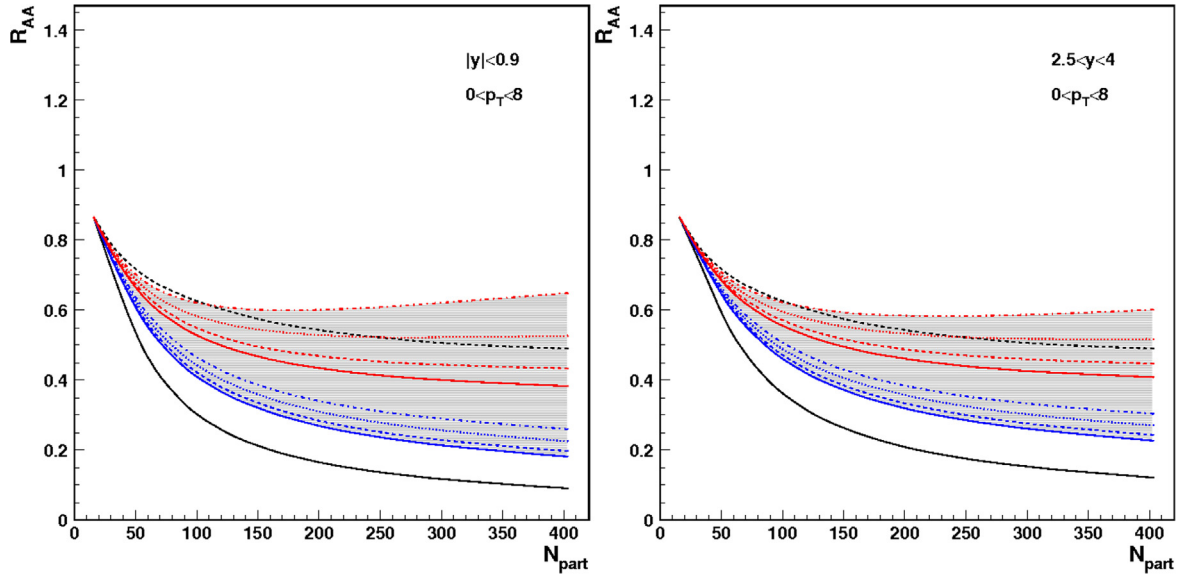


**Fig. 6.** (Color online.) Results on the centrality dependence of the  $J/\psi$  nuclear modification factor in PbPb collisions at 5.5 TeV at mid (left) and forward (right) rapidity. The dashed black line corresponds to the shadowing effect on the  $J/\psi$ . The lowest continuous line (black) corresponds to the combined effect of the shadowing and the comover dissociation. The shadowed area corresponds to our result when the shadowing, the comover dissociation and the recombination are taken into account. The uncertainty takes into account the variation between the minimum (blue line) and maximal (red line) values of  $C(y)$ . For the mid-rapidity region, we have taken, from down to up,  $\frac{d\sigma_{pp}^{c\bar{c}}}{dy} = 0.8, 0.85, 0.9, 0.95, 1.0, 1.1, 1.15$  mb and for the forward rapidity region  $\frac{d\sigma_{pp}^{c\bar{c}}}{dy} = 0.65, 0.67, 0.71, 0.74, 0.82, 0.84, 0.87, 0.89$  mb.

The data in this region agrees with this choice in the interval  $2.5 < y < 3.5$ , while for the most forward points an scenario with smaller amount of recombination or only dissociation without recombination is clearly favored. Note that the lower curve in the right-hand side of Fig. 5 corresponds to the behavior of the comover dissociation, whose amount decreases rapidly when going from 2 to 4 in the rapidity range. More realistic  $y$ -dependent value of  $C(y)$  could modify these curves.

We finish by presenting our predictions for the LHC energy of 5.5 TeV. Here we have let vary our  $C(y)$ -value between 2 and 4. Taking  $BR_{ll} \times \frac{d\sigma_{pp}^{J/\psi}}{dy}|_{y=0} \approx 350$  nb [37] and  $\sigma_{pp} = 60$  mb,

these  $C(y)$ -values correspond to an input charm cross section  $\frac{d\sigma_{pp}^{c\bar{c}}}{dy} \approx 0.8\text{--}1.15$  mb in the mid-rapidity region. In the rapidity range  $2.5 < y < 4$  we take a mean reduction in the  $C(y)$ -value of the order of 20%, which corresponds to an input charm cross section  $\frac{d\sigma_{pp}^{c\bar{c}}}{dy} \approx 0.6\text{--}0.9$  mb when  $BR_{ll} \times \frac{d\sigma_{pp}^{J/\psi}}{dy} \approx 250$  nb [37]. Our results in the mid and forward rapidity ranges are plotted in Fig. 6.

Note that in the previous work [16] stronger shadowing corrections – of around 20% larger than the present ones – for the heavy quark production were considered, which implied both less recombination effects and stronger total suppression. This demonstrates that the implementation of the initial-state effects is more relevant

than what is currently assumed in the recombination approaches, since it affects the probability of regeneration.

#### 4. Conclusion

In this work we have studied the combined effect of  $J/\psi$  dissociation and recombination of  $c\bar{c}$  pairs into  $J/\psi$  in the comover interaction model. This model does not assume thermal equilibrium of the matter produced in the collision and includes a comprehensive treatment of initial-state effects, such as shadowing. We estimate the magnitude of the recombination term from  $J/\psi$  and open charm yields in  $pp$  collisions at LHC. Without any adjustable parameters, the centrality, transverse momentum and rapidity dependence of experimental data is reproduced.

In our approach, the magnitude of the recombination effect is controlled by the total charm cross section in  $pp$  collisions. Note that, contrary to the results in [16], where the combined effect of initial-state shadowing and comover dissociation appeared to overcome the effect of parton recombination at 5.5 TeV, we find here that the recombination effects are of crucial importance in PbPb collisions at LHC energies and can dominate over the suppression, in agreement with [44,43,51]. The reason for this discrepancy is the fact that a different approach for the shadowing factor for heavy quark production was used in [16], which minimized the amount of recombination and led to an overestimation of the total suppression.

Let us finish by an important remark: we are aware that the comover interaction model at these energies should not be considered to describe a final-state interaction at the hadronic level. Indeed, at small values of the proper time these comovers should be considered as a dense partonic medium. A large contribution to the comover interaction comes from the few first fm/c, where the system is in partonic or pre-hadronic stage. The comover interaction cross section used here, averaged over time, do not distinguish between these two scenarios. A more refined study would consist on the introduction of different comover interaction cross sections, that could vary with the proper time or the densities – using the inverse proportionality between proper time and densities. The advantage of the present approach is the economy of parameters and the simplicity of the equations, that can be, at least partially, analytically resolved.

#### Acknowledgements

It is a pleasure to thank R. Arnaldi, A. Capella, F. Fleuret, J.-P. Lansberg and E. Scapparini for useful exchanges. This work was partially supported by the Ministerio de Ciencia (Spain) and the IN2P3 (France) (AIC-D-2011-0740).

#### References

- [1] T. Matsui, H. Satz, Phys. Lett. B 178 (1986) 416.
- [2] B. Alessandro, et al., Eur. Phys. J. C 39 (2005) 335.
- [3] A. Capella, A. Kaidalov, A. Kouider Akil, C. Gerschel, Phys. Lett. B 393 (1997) 431.
- [4] N. Armesto, A. Capella, Phys. Lett. B 430 (1998) 23.
- [5] N. Armesto, A. Capella, E.G. Ferreiro, Phys. Rev. C 59 (1999) 395.
- [6] A. Capella, E.G. Ferreiro, A.B. Kaidalov, Phys. Rev. Lett. 85 (2000) 2080.
- [7] R. Thews, M. Schroedter, J. Rafelski, Phys. Rev. C 63 (2001) 054905.
- [8] L. Grandchamp, R. Rapp, Nucl. Phys. A 709 (2002) 415.
- [9] L. Yan, P. Zhuang, N. Xu, Phys. Rev. Lett. 97 (2006) 232301.
- [10] P. Braun-Munzinger, J. Stachel, Phys. Lett. B 490 (2000) 196.
- [11] A. Andronic, P. Braun-Munzinger, K. Redlich, J. Stachel, Phys. Lett. B 571 (2003) 36.
- [12] A.P. Kostyuk, M.I. Gorenstein, H. Stöcker, W. Greiner, Phys. Rev. C 68 (2003) 041902.
- [13] A. Capella, E.G. Ferreiro, Eur. Phys. J. C 42 (2005) 419.
- [14] A. Adare, et al., Phys. Rev. Lett. 98 (2007) 232301.
- [15] M.J. Leitch, J. Phys. G 34 (2007) S453.
- [16] A. Capella, L. Bravina, E.G. Ferreiro, A.B. Kaidalov, K. Tywoniuk, E. Zabrodin, Eur. Phys. J. C 58 (2008) 437.
- [17] C.W. De Jager, H. De Vries, C. De Vries, At. Data Nucl. Data Tables 14 (1974) 479.
- [18] M.A. Braun, C. Pajares, C.A. Salgado, N. Armesto, A. Capella, Nucl. Phys. B 509 (1998) 357.
- [19] A. Capella, E.G. Ferreiro, Phys. Rev. C 76 (2007) 064906.
- [20] C. Lourenco, R. Vogt, H.K. Woehri, J. High Energy Phys. 0902 (2009) 014.
- [21] V.N. Gribov, Sov. Phys. JETP 29 (1969) 483; V.N. Gribov, Sov. Phys. JETP 30 (1970) 709; V.N. Gribov, Sov. Phys. JETP 26 (1968) 414.
- [22] A. Schwimmer, Nucl. Phys. B 94 (1975) 445.
- [23] A. Capella, A. Kaidalov, J. Tran Thanh Van, Acta Phys. Hung., Heavy Ion Phys. 9 (1999) 169.
- [24] N. Armesto, A. Capella, A.B. Kaidalov, J. Lopez-Albacete, C.A. Salgado, Eur. Phys. J. C 29 (2003) 531.
- [25] A. Capella, D. Sousa, Phys. Lett. B 511 (2001) 185.
- [26] A. Capella, E.G. Ferreiro, Eur. Phys. J. C 72 (2012) 1936.
- [27] E.G. Ferreiro, F. Fleuret, J.P. Lansberg, A. Rakotozafindrabe, Phys. Lett. B 680 (2009) 50.
- [28] A. Rakotozafindrabe, E.G. Ferreiro, F. Fleuret, J.P. Lansberg, N. Matagne, Nucl. Phys. A 855 (2011) 327.
- [29] E.G. Ferreiro, Contribution to Rencontres de Moriond 2008: QCD and high energy interactions, arXiv:0805.2753 [hep-ph].
- [30] E.G. Ferreiro, F. Fleuret, J.P. Lansberg, A. Rakotozafindrabe, Contribution to Rencontres de Moriond 2009: QCD and high energy interactions, arXiv:0903.4908 [hep-ph].
- [31] R. Vogt, Phys. Rev. C 81 (2010) 044903.
- [32] S. Brodsky, A.H. Mueller, Phys. Lett. B 206 (1988) 685.
- [33] B. Koch, U. Heinz, J. Pitsut, Phys. Lett. 243 (1990) 149.
- [34] A. Capella, Phys. Lett. B 364 (1995) 175.
- [35] A. Capella, A. Kaidalov, A. Kouider Akil, C. Merino, J. Tran Thanh Van, Z. Phys. C 70 (1996) 507; A. Capella, C.A. Salgado, D. Sousa, Eur. Phys. J. C 30 (2003) 111.
- [36] B. Abelev, et al., ALICE Collaboration, Phys. Lett. B 718 (2012) 295.
- [37] F. Bossu, Z.C. del Valle, A. de Falco, M. Gagliardi, S. Grigoryan, G. Martinez Garcia, arXiv:1103.2394 [nucl-ex].
- [38] B. Abelev, ALICE Collaboration, J. High Energy Phys. 1207 (2012) 191.
- [39] B. Abelev, et al., ALICE Collaboration, Phys. Rev. Lett. 109 (2012) 072301.
- [40] J. Wiechula, ALICE Collaboration, arXiv:1208.6566 [hep-ex].
- [41] E. Scapparini, ALICE Collaboration, Nucl. Phys. A 904–905 (2013) 202c; I.-C. Arsene, ALICE Collaboration, Nucl. Phys. A 904–905 (2013) 623c.
- [42] R. Arnaldi, ALICE Collaboration, Nucl. Phys. A 904–905 (2013) 595c.
- [43] X. Zhao, R. Rapp, Nucl. Phys. A 859 (2011) 114.
- [44] A. Andronic, P. Braun-Munzinger, K. Redlich, J. Stachel, J. Phys. G 38 (2011) 124081.
- [45] E.G. Ferreiro, F. Fleuret, J.P. Lansberg, A. Rakotozafindrabe, Phys. Rev. C 88 (2013) 047901.
- [46] A. Capella, E.G. Ferreiro, Phys. Rev. C 75 (2007) 024905.
- [47] A. Capella, E.G. Ferreiro, in preparation.
- [48] S. Chatrchyan, et al., CMS Collaboration, J. High Energy Phys. 1205 (2012) 063.
- [49] C. Mironov, CMS Collaboration, Contribution to Quark Matter 2012, Nucl. Phys. A 904–905 (2013) 194c.
- [50] D.H. Moon, CMS Collaboration, Contribution to Quark Matter 2012, Nucl. Phys. A 904–905 (2013) 591c.
- [51] Y.-p. Liu, Z. Qu, N. Xu, P.-f. Zhuang, Phys. Lett. B 678 (2009) 72.